

Latest results from the DAMPE space mission

Irene Cagnoli^{1,2}, *Ivan De Mitri*^{1,2*}, and *Leandro Silveri*^{1,2}
on behalf of the DAMPE collaboration

¹Gran Sasso Science Institute (GSSI), L'Aquila, Italy

²Istituto Nazionale di Fisica Nucleare (INFN)—Laboratori Nazionali del Gran Sasso, L'Aquila, Italy

Abstract. The space-based DAMPE (DARk Matter Particle Explorer) particle detector has been taking data for more than 7 years since its successful launch in December 2015. Its main scientific goals include the indirect search for dark matter signatures in the cosmic lepton and gamma-ray spectra, the study of galactic cosmic rays up to energies of hundreds of TeV and studies on high-energy gamma ray astronomy. The measurement of galactic cosmic ray spectra are reported here, those being fundamental tools to investigate the mechanisms of acceleration at their sources and propagation through the interstellar medium. Results on proton and helium, which revealed new spectral features, are described. Ongoing analyses on the cosmic ray light, medium and heavy mass nuclei are outlined, together with studies of the so-called secondary cosmic rays. Latest results on gamma-ray astronomy and dark matter search will be also summarized.

1 Introduction

The DARk Matter Particle Explorer [1] (DAMPE) is a space particle detector, launched on 17 December 2015 by a collaboration of Chinese, Italian and Swiss scientific institutions. It is operating in a sun-synchronous orbit at an altitude of ~ 500 km, with an inclination of $\sim 97^\circ$ and a period of about 95 minutes. The total mass of the payload is about 1400 kg with a power consumption of about 400 W.

The main scientific objectives of the DAMPE space mission are the indirect search for dark matter (DM) signatures, the high energy gamma ray astronomy, the study of cosmic electron + positron spectrum and the study of cosmic ray protons and nuclei. Therefore, the DAMPE detector is designed to have excellent performances for the detection of cosmic electrons and photons in the energy range from 10 GeV to 10 TeV and to measure the fluxes and the mass composition of galactic cosmic ray nuclei from 50 GeV up to hundreds of TeV. In particular, it is characterised by a large acceptance, corresponding to $0.3 \text{ m}^2 \text{ sr}$ for electrons above 30 GeV, and an accurate angular resolution for electrons and photons that is less than 0.2° with $\sim 0.1 \text{ sr}$ of field of view. Moreover, it has an excellent energy resolution, being 1.2% for electrons at 100 GeV and below 40% for nuclei at 800 GeV [1].

*e-mail: ivan.demitri@gssi.it

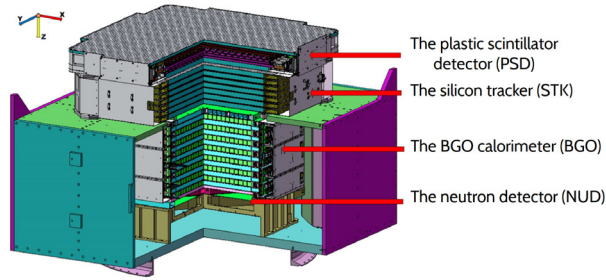


Figure 1: Schematic view of the DAMPE detector with subdetector modules.

2 The DAMPE detector

The detector consists of four subdetector modules which are, from top to bottom, a Plastic Scintillator Detector (PSD), a Silicon-Tungsten tracker converter (STK), a BGO calorimeter and a NeUtron Detector (NUD), shown in figure 1.

The PSD [2] is designed to measure the absolute value of the charge of incident cosmic rays (CRs) up to iron and acts also as an anti-coincidence detector for γ -ray observations. It is composed of 2 planes, oriented respectively in x and y directions, having 41 plastic scintillator bars each. The bars are disposed in 2 staggered layers to increase the hermeticity and readout by 2 photomultiplier tubes (PMTs).

The STK [3] operates to reconstruct the trajectory of the incident particles. It has 6 x-y tracking planes of silicon microstrip detectors that provide independent particle coordinate measurements in the two orthogonal directions perpendicular to the telescope pointing direction. To promote the photon conversion, 3 tungsten layers (1 mm thick) are inserted after the first, second and third tracking planes.

The calorimeter [4] is made of 14 layers of bismuth germanium oxide (BGO) bars and it is characterised by a total depth of ~ 32 radiation lengths and ~ 1.6 nuclear interaction lengths. It is designed to measure the energy of incident particles and to provide efficient electromagnetic/hadronic showers discrimination. For this reason the layers are in a hodoscopic configuration to perform a 3D imaging of the shower profiles and they are composed of 22 BGO bars ($2.5 \times 2.5 \times 60 \text{ cm}^3$) readout by PMTs on the two ends.

The NUD [5] detects the secondary neutrons within few μs after their production in the BGO, thus improving the electron/hadron separation power.

2.1 Beam tests at CERN and on-orbit calibration

Several beam test campaigns had been performed at CERN, between 2014 and 2015 [1] to validate the detector performances and to determine the calibration parameters. Different particle beams had been used, namely electrons, photons, pions, protons and nuclear fragments. Then, in the first two weeks after the DAMPE launch a dedicated calibration was performed using cosmic rays and the results were compared with those obtained in the beam tests at CERN to verify the on-orbit performance of the detector. Furthermore, in order to ensure good quality of the energy and charge measurements for individual events, the detection efficiency and to check the stability of the detector, a calibration of each sub-detector is periodically performed during the on-orbit operation [6]. In particular, twice per orbit the DAQ system collects 40 s of data for the electronic linearity and the pedestal calibration.

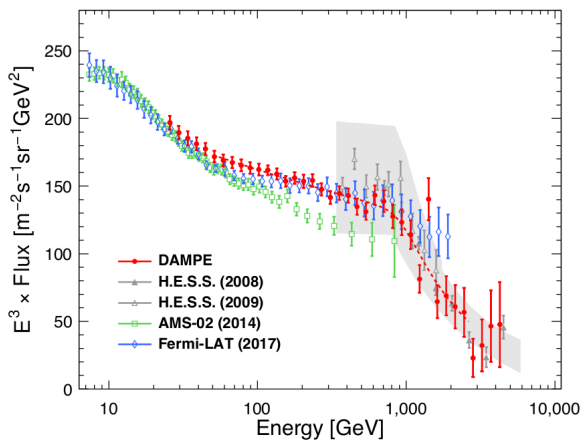


Figure 2: DAMPE CRE spectrum (red markers) multiplied by E^3 , compared with measurements from other experiments. The error bars include both the systematic and the statistical uncertainties added in quadrature. The red dashed line represents the smoothly broken power law fit [7].

While, other calibrations, including the minimum ionization particle response and detector alignment, are performed using the nominal science data.

3 Results and ongoing analyses

3.1 All-electron ($e^+ + e^-$) spectrum

One of the main goals of the experiment is the measurement of the cosmic ray electron plus positron (CRE) spectrum, since it dispenses a probe for the study of Galactic high energy processes and it could enable the indirect dark matter observation. DAMPE performed this measurement between 25 GeV and 4.6 TeV using 530 days of data [7]. The electron-positron sample was selected with a high purity thanks to the efficient electromagnetic/hadronic shower discrimination provided by the BGO calorimeter.

The selection relies on the differences in the transverse spread of the shower produced and in the ratio between the energy deposited in the last layer and the total energy released in the calorimeter. Applying this method a proton rejection efficiency of 99.99% has been obtained keeping the electron efficiency at 90%, with a discrimination factor of 10^5 - 10^6 [7].

The CRE spectrum, shown in figure 2, exhibits a spectral hardening at ~ 50 GeV in agreement with AMS-02 [8] and Fermi-LAT[9] and provides a first direct and clear detection of a break at about 0.9 TeV, confirming with high precision the feature previously observed by H.E.S.S. [10]. The measured CRE spectrum in the 55 GeV - 2.63 TeV energy range is properly fitted using a smoothly broken power law model, instead of a unique power law. Hence, the spectral index is found to change from ~ 3.1 to ~ 3.9 at the ~ 0.9 TeV spectral break. This study will be pursued including the updated spectrum with larger statistics as well as a more powerful background rejection via the implementation of machine learning algorithms [11], thus extending the analysis to higher energies.

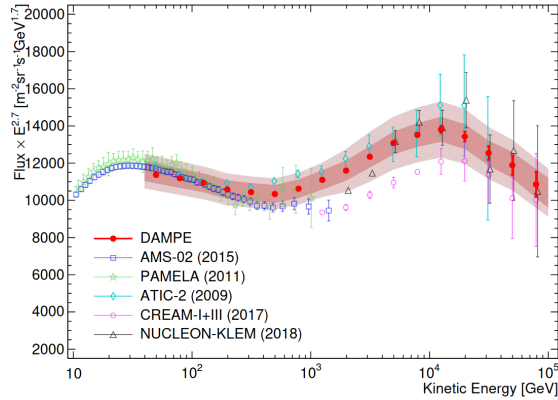


Figure 3: DAMPE proton spectrum (red dots) from 40 GeV to 100 TeV, compared with measurements from other experiments [13–15, 19, 20]. The red error bars refer to the statistical uncertainties. The inner band shows the estimated systematic uncertainties, the outer band refers to the total systematic uncertainties including also those from the hadronic models. The error bars of PAMELA and AMS-02 data include both statistical and systematic uncertainties added in quadrature, while for ATIC, CREAM, and NUCLEON data only statistical uncertainties are shown [12].

3.2 Proton spectrum

The DAMPE detector measured the proton spectrum in the 40 GeV - 100 TeV energy range using its first 30 months of data [12]. The background rejection was performed by using the previously described calorimetric analysis to reject the background contribution due to electrons and positrons, and thanks to the charge selection performed by the PSD, helium and heavier nuclei were discarded. Moreover, a Monte Carlo (MC) based correction that estimated the remaining fraction of helium, after background rejection, was applied.

The obtained proton spectrum (see figure 3) is characterized by a hardening at few hundreds of GeV, previously observed by other experiments [13–18], and revealed a softening at ~ 14 TeV with a significance of 4.7σ . These spectral breaks show that above the hardening the spectrum is more accurately described by a smoothly broken power law model and from the fit the spectral index changes from ~ 2.60 to ~ 2.85 at ~ 13.6 TeV [12].

3.3 Helium spectrum

The DAMPE helium spectrum, reported in figure 4, was measured in the 70 GeV -80 TeV energy range using 54 months of data. It is characterized by a behaviour similar to the proton spectrum. In fact, it shows an hardening at ~ 1 TeV, confirming the previous results observed by other experiments [22–26], and at ~ 34 TeV it has a softening with high significance, 4.3σ [21]. For the selection of the He data, the charge measured with the PSD was used. Moreover, also the information from the first plane of the STK tracker was included in the analysis to improve the proton background rejection.

The comparison between the proton flux and helium flux data offers the possibility to get new insights into the acceleration and propagation mechanisms; in particular, the different position of the softening in the proton and He spectra suggests that this feature could be rigidity-dependent, albeit, due to the measurement uncertainties, the hypothesis of a mass-dependent softening cannot be excluded.

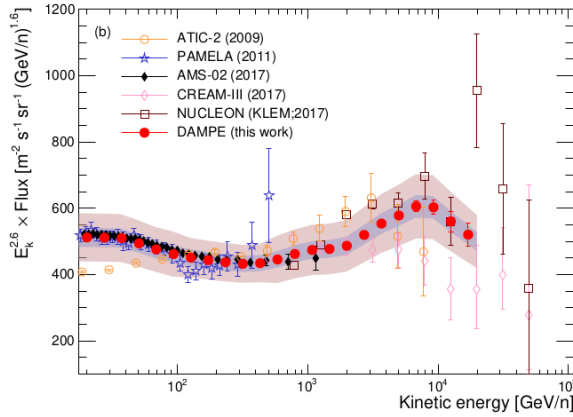


Figure 4: DAMPE He spectrum in kinetic energy per nucleon compared with measurements from other experiments [22, 23, 25, 26]. The red error bars refer to the statistical uncertainties. The inner band shows the estimated systematic uncertainties, the outer band refers to the total systematic uncertainties including also those from the hadronic models [21].

3.4 p+He spectrum

The DAMPE experiment measured also the p+He energy spectrum up to hundreds of TeV [27]. Thanks to the much lower fluxes of the other light nuclei, the sample was selected with larger efficiency and larger purity than the analyses with proton or helium alone. Moreover, looser analysis cuts have been applied allowing to have very high statistics and to cover a more extended energy range. This enables to compare the high energy part of the obtained spectrum with the measurements performed with ground-based experiments. In figure 5 the spectrum obtained with a preliminary analysis is shown. It ranges up to ~150 TeV and is characterized by a hardening at ~600 GeV and a softening at ~25 TeV [27]. This analysis

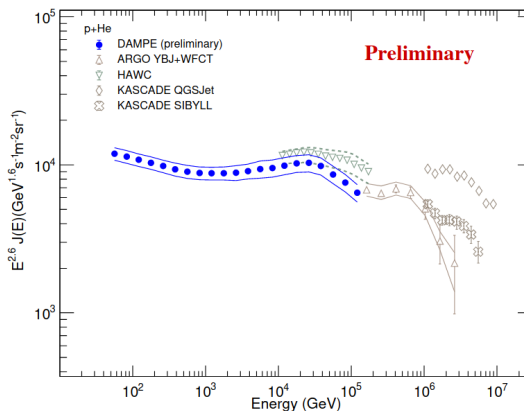


Figure 5: DAMPE p + He spectrum (red dots) weighted by $E^{2.6}$ [27], compared with indirect measurements from other experiments [28–30].

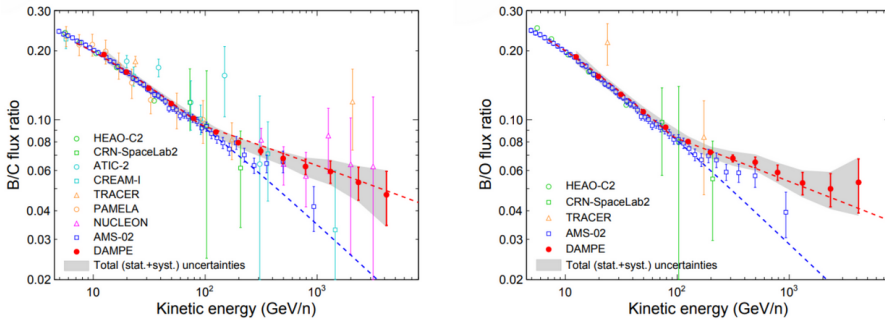


Figure 6: The DAMPE boron to carbon (left) and boron to oxygen (right) flux ratios as a function of kinetic energy per nucleon [31], compared with the measurements from other experiments. The red error bars refer to the statistical uncertainties. The shaded band shows the total systematic uncertainties including those from the hadronic models.

is now being finalized in order to extend the energy range to higher energies and include a complete evaluation of the systematic uncertainty.

3.5 Heavier nuclei

There are various ongoing analyses on heavier nuclei that are studying the secondaries Li and Be, the independent spectra of B, C and O, as well as the boron to carbon (B/C) and boron to oxygen (B/O) flux ratios, and heavier nuclei such as Ne, Mg, Si, up to Fe.

Recent results [31] have been obtained for the secondary-to-primary ratios B/C and B/O, which are of particular interest since boron nuclei are thought to be mainly of secondary origin and to be produced from the fragmentation of heavier primary nuclei, such as carbon and oxygen. Therefore, the measurement of these flux ratios provide information about the CR acceleration and propagation in the Galaxy. The B/C and B/O flux ratios have been measured in the range between 10 GeV/n and 5.6 TeV/n using six years of data. In both cases, a spectral hardening has been observed at ~ 100 GeV/n as it is shown in figure 6.

3.6 Gamma-ray astronomy and dark matter searches

Gamma-ray analysis was performed by the DAMPE experiment with high precision thanks to its excellent energy and angular resolutions, corresponding to $\sim 1\%$ and $\sim 0.1^\circ$ at 100 GeV, respectively. The photon events selection was performed using the information from the PSD in order to veto the charged particle events. Moreover, the topology of the shower in the calorimeter was studied to further suppress the proton background component and the STK signal from the first plane was used to reject the surviving electron events.

An analysis for the detection of high energy gamma-ray sources was performed using 5 years of data [32]. A sky map (see figure 7) was produced and it is characterized by 222 identified γ -ray sources which were also associated to the Fermi catalog (4FGL) [33], leading to the identification of several active galactic nuclei and pulsars.

Moreover, the DAMPE gamma-ray studies include the search for sharp line-like features in the photon spectrum [34], since peaked emission lines, if detected, are unlike to be produced by known astrophysical processes and according to some DM models they might be originated from a process involving a DM particle. A search for γ -ray lines was performed

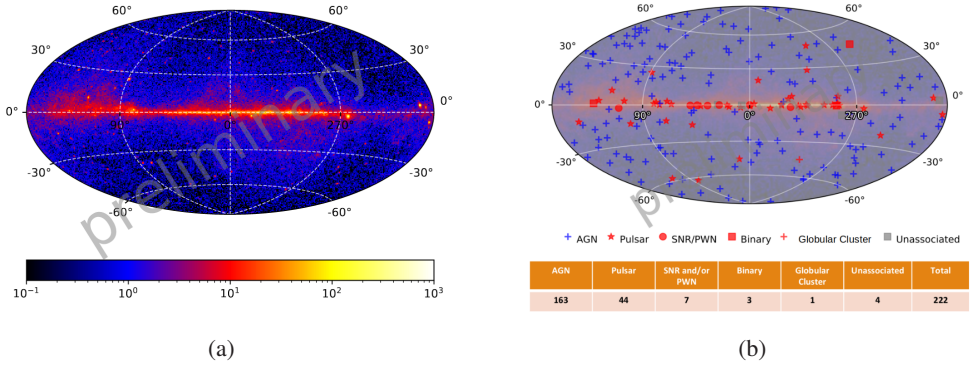


Figure 7: Preliminary sky map (a) and Gamma-ray sources (b) in association with 4FGL observed by DAMPE [32].

using 5 years of data in the 10 - 300 GeV energy range. Since no line signals were detected, a 95% of confidence level constraint was put on the DM decay lifetime and annihilation cross section, as shown in figure 8.

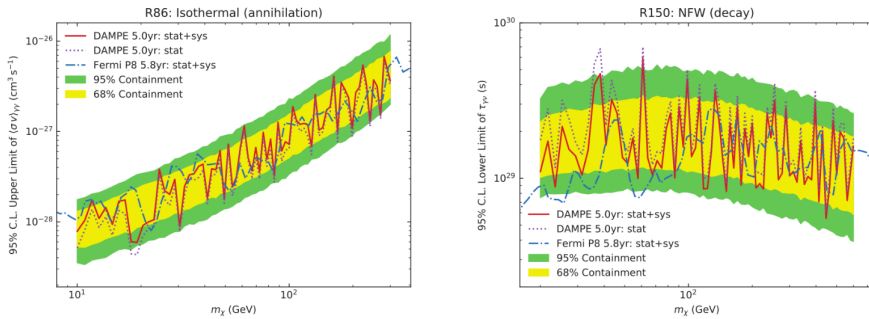


Figure 8: Limits from gamma line searches by DAMPE. A 95% confidence level constraints for different DM models. In the left panel, upper limits on the velocity-averaged annihilation cross-section for DM annihilation are shown. In the right panel the lower limits on the DM decay lifetime are illustrated. The yellow and green bands refer to the 68% and 95% containment respectively [34].

4 Conclusions

The DAMPE detector is operating since December 2015 and in these years of data taking it obtained several results. The electron-positron spectrum was observed over a wide energy range up to 4.6 TeV, providing a first direct and clear detection of a break at about 0.9 TeV. Moreover, the proton and He spectra have been measured up to 100 TeV and up to 80 TeV respectively. In both spectra a hardening at hundreds of GeV/n was confirmed, and for the first time DAMPE revealed a spectral softening at ~ 14 TeV for protons and at ~ 34 TeV for He. A preliminary $p + \text{He}$ combined spectrum was also been measured in an energy range that extends to higher energies with respect to the independent spectra with the single elements,

allowing for a comparison with ground-based experiments results. Other ongoing analyses are focusing on the measurement of primary and secondary CR spectra and recently a study on the B/C and B/O flux ratios was published, showing a hardening at ~ 100 GeV/n for both flux ratios giving new insight into acceleration and propagation mechanisms of CRs in our Galaxy. In addition, using the first five years of data, DAMPE produced a gamma-ray sky map with the identification of 222 sources, also setting upper limits on the cross section of DM annihilation from gamma line searches.

References

- [1] J. Chang et al., *Astropart. Phys.* (95), 6-24 (2017)
- [2] Y. Yu et al., *Astropart. Phys.* (94), 1-10 (2017)
- [3] P. Azzarello et al., *Nucl. Instrum. Methods Phys. Res. Sect. A* (831), 378 (2016)
- [4] Z. Zhang et al., *Nucl. Instrum. Methods Phys. Res. Sect. A* (836), 98 (2016)
- [5] Y-Y. Huang et al., *Res. Astrophys.* (20), 153 (2020)
- [6] G. Ambrosi et al., *Astropart. Phys.* (106), 18-34 (2019)
- [7] G. Ambrosi et al., *Nature* (552), 63-66 (2017)
- [8] M. Aguilar et al., *Phys. Rev. Lett.*(113), 121 102 (2014)
- [9] S. Abdollahi et al., *Phys. Rev. D* (95), 082007 (2017)
- [10] F. Aharonian et al., *Phys. Rev. Lett.* (101), 261 104 (2008)
- [11] D. Droz et al., *JINST* (16), P07036 (2021)
- [12] Q. An et al., *Science Advances* (5), eaax3793 (2019)
- [13] A. D. Panov, et al., *Bull. Russ. Acad. of Sci.: Phys.* (73), 564-567 (2009)
- [14] O. Adriani et al., *Science* (332), 69 (2011)
- [15] M. Aguilar et al., *Phys. Rev. Lett.* (114), 171103 (2015)
- [16] O. Adriani et al., *Phys. Rev. Lett.* (122), 181102 (2019)
- [17] Y. S. Yoon et al., *Astrophys. J.* (839), 5 (2017)
- [18] E. Atkin et al., *Astropart. Phys.* (90), 69 (2017)
- [19] M. Aguilar et al., *Phys. Rev. Lett.* (119), 251101 (2017)
- [20] E. Atkin et al., *JETP Lett.* (108), 5-12 (2018)
- [21] F. Alemanno et al., *Phys. Rev. Lett.* (126), 201102 (2021)
- [22] O. Adriani et al., *Science* (332), 69 (2011)
- [23] A. D. Panov et al., *Bull. Russ. Acad. Sci.: Phys.* (73), 564 (2009)
- [24] Y. S. Yoon et al., *Astrophys. J.* (839), 5 (2017)
- [25] M. Aguilar et al., *Phys. Rev. Lett.* (115), 211101 (2015)
- [26] E. Atkin et al., *J. Cosmol. Astropart. Phys.* (07), 020 (2017)
- [27] F. Alemanno et al., *PoS (ICRC2021)*, 117 (2021)
- [28] A. Albert et al., *Phys. Rev. D* (105), 063021 (2022)
- [29] B. Bartoli et al. *Phys. Rev. D* (92), 092005 (2015)
- [30] K. H. Kampert et al. *Acta Phys. Pol. B* (35), 1799 (2004)
- [31] F. Alemanno et al., *Science Bulletin* (67), 2162-2166 (2022)
- [32] K.-K. Duan et al., *PoS (ICRC2021)*, 631(2021)
- [33] S. Abdollahi et al.,*Astrophys.J.Supp.* (247), 33 (2020)
- [34] F. Alemanno et al., *Science Bulletin* (67), 679-684 (2022)